

## Adsorption of Direct Red 80 dye from aqueous solution onto almond shells: Effect of pH, initial concentration and shell type

F. Doulati Ardejani<sup>a,b,\*</sup>, Kh. Badii<sup>b</sup>, N. Yousefi Limaee<sup>b</sup>, S.Z. Shafaei<sup>a,b</sup>, A.R. Mirhabibi<sup>b,c</sup>

<sup>a</sup> Faculty of Mining and Geophysics, Shahrood University of Technology, Shahrood, Iran

<sup>b</sup> Environmental Science and Engineering Department, Iran Colour Research Centre, Tehran, Iran

<sup>c</sup> Department of Metallurgy, University of Science and Technology of Iran, Tehran, Iran

Received 19 September 2006; received in revised form 13 June 2007; accepted 13 June 2007

Available online 17 June 2007

### Abstract

The adsorption of Direct Red 80 (DR 80) dye from aqueous solution on almond shells as an eco-friendly and low-cost adsorbent was studied. The effect of shell type (internal, external and mixture shells), pH and initial dye concentration were considered to evaluate the sorption capacity of almond shell adsorbent. The mixture type of almond shell showed to be more effective. The adsorption studies revealed that the mixture type of almond shells remove about 97% of the DR 80 dye from aqueous phase after 1 h of the adsorption process in a batch system. Although, pH changes did not appreciably affect the adsorption process but the maximum adsorption capacity of different types of almond shells (20.5, 16.96 and 16.4 mg/g for mixture, external and internal shells) were obtained at pH 2. However, in order to have a better control on the experimental conditions, pH 6 was selected for conducting all adsorption experiments. Initial dye concentration was varied from 50 to 150 mg/L. Higher concentrations of dye in aqueous solution reduced DR 80 dye adsorption efficiency of almond shells. Equilibrium data were attempted by various adsorption isotherms including Langmuir, Freundlich and Brunauer–Emmett–Teller (BET) models. It was found that the adsorption process by mixture type of almond shells follows the Langmuir non-linear isotherm. Furthermore, the experimental data by internal and external almond shells could be well described by the BET and Freundlich isotherm models, respectively. The pseudo-second-order kinetics provides the best correlation of the experimental data.

© 2007 Elsevier B.V. All rights reserved.

**Keywords:** Direct Red 80 (DR 80); Adsorption; Almond shells; Isotherm; Kinetics; Aqueous solution

### 1. Introduction

The textile industry is responsible to produce a large volume of polluted effluents discharging to the receiving environment. Synthetic dyes are recognised to be the most important hazardous material found in textile effluents which need to be removed. Because the presence of dyes in effluents cause many damage to the ecological system of the receiving surface water [1,2] and create a lot of disturbance to the groundwater resources. The industrial effluents containing dyes reduce light penetration, preventing the photosynthesis of aqueous flora [3]. Some dyes may cause allergy, skin irritation and cancer to humans. In order to minimise the risk of pollution problems from such effluents, it is necessary to accurately treat them before discharging to

the environment. Substantial attempts have been made by many researchers to find suitable treatment systems in order to treat wastes discharged from different industries in particular textile industry [1,2,4–12].

A wide range of chemical and physical procedures of dyes removal from aqueous solutions is based on the decolourization by photocatalytic degradation [7,12,13], membranes [14], microbiological decomposition [15], electrochemical oxidation of dye [16] and adsorption techniques [3,8,9,11,17–19]. From all these techniques for dye removal from industrial effluents, the adsorption process is noted to be superior because it is economically cost effective, efficient [8] and simple [2]. This method was widely used for the treatment of industrial effluents containing colour, heavy metals and other organic and inorganic hazardous impurities [11]. Using adsorption process the hazardous dye is transferred from the aqueous phase to a solid phase. Besides that, the microbiological, photocatalytic and electrochemical decomposition procedures are not efficient because many dyes

\* Corresponding author at: Tel.: +98 273 3335509; fax: +98 273 3335509.  
E-mail address: [fdoulati@shahrood.ac.ir](mailto:fdoulati@shahrood.ac.ir) (F. Doulati Ardejani).

Table 1  
Comparison of the adsorption capacities of various adsorbents used for dye removal from aqueous solutions

Adsorbent	Dye	Maximum adsorption capacity (mg/g)	Source
Mixture almond shells	Direct Red 80	22.422	Present study
Compost	Acid Black 24	86	[2]
Compost	Acid Orange 74	15	[2]
Compost	Basic Blue 9	200	[2]
Compost	Basic Green 4	69.4	[2]
Compost	Direct Blue 71	22	[2]
Compost	Direct Orange 39	17	[2]
Compost	Reactive Orange 16	9	[2]
Compost	Reactive Red 2	20	[2]
Peanut hull	Amaranth	14.90	[3]
Peanut hull	Sunset Yellow	13.99	[3]
Peanut hull	Fast Green FCF	15.60	[3]
Lignite coal	C.I. Acid Red 88	30.9	[4]
Bituminous coal	C.I. Acid Red 88	26.1	[4]
Orange peel	Direct Red 23	10.718	[19]
Orange peel	Direct Red 80	21.052	[19]
Fungus <i>Aspergillus niger</i>	Congo Red	14.72	[23]
Soy meal hull	Direct Red 80	178.57	[24]
Soy meal hull	Direct Red 81	120.48	[24]
Soy meal hull	Acid Blue 92	114.94	[24]
Soy meal hull	Acid Red 14	109.89	[24]
Flyash	Methylene Blue	4.48	[31]
Pyrophyllite	Methylene Blue	70.42	[32]
Pyrophyllite	Procion Crimson H-EXL	71.43	[32]

cannot be easily decomposed [13,16]. Furthermore, the high cost of activated carbon sometimes limits its applicability for dye removal [11,18]. Therefore, there is a growing interest to search for alternative materials, which are relatively cost effective and at the same time having high adsorption efficiency [11]. These research works include use of wood and saw dust [11,20], fly ash [21], wheat straw [22], apple pomace [22], fungus [23] and orange peels [19], soy meal hull [24], eggshell membrane [25], etc. Table 1 compares the adsorption capacities of various materials including almond shell used in this study.

Most of the research works on almond shell are limited to its use as source of activated carbon [26,27]. Almond shell was used to remove pentachlorophenol from aqueous matrices [28] and has not been previously used as an adsorbent for the removal of textile dyes from aqueous solutions.

In the present study, almond shells are used to remove DR 80 dye from the aqueous solution. Equilibrium data are attempted by various adsorption isotherms including Langmuir, Freundlich and Brunauer–Emmett–Teller (BET) [29] isotherms in order to select an appropriate isotherm model. A kinetics study of the adsorption process is also considered in the present study to describe the rate of sorption.

## 2. Experimental

### 2.1. Preparation of adsorbent

The almond shells were obtained from a local fruit field in east north of Iran. The almond shells were first washed to remove any adhering dirt and then were dried. The material was sieved

in the mineral processing laboratory at Shahrood University of Technology to obtain the particle size of <106  $\mu\text{m}$ .

### 2.2. Reagents and solutions

DR 80 dye was obtained from Ciba Ltd. and was used without further purification. The chemical structure of this dye is shown in Fig. 1. Distilled water was throughout employed as solvent. Working solution of 50 mg/L was prepared. The pH adjustments of the solution were made by adding a small amount of HCl or NaOH (1M).

### 2.3. Adsorption procedure

The adsorption measurements were conducted by mixing various amounts of almond shells (0.05–0.8 g) in jars containing 250 mL of a dye solution (50 mg/L) and 5 g NaCl at pH 6, an agitating speed of 200 rpm and temperature 20 °C for 300 min to attain equilibrium conditions. An FC6S-VELP (Scientifica) jar test was used for agitating purpose. Different agitation rates ranging from 30 to 200 rpm had no significant change on adsorption process. The changes of absorbance were determined at certain time intervals (2, 4, 6, 8, 10, 20, 30, 60, 120, 180, 240 and 300 min) during the adsorption process. After adsorption experiments, the sorbent were separated from the solution by Hettich EBA20 centrifuge and dye concentration was then determined. The results were evaluated by various adsorption isotherms incorporating Langmuir, Freundlich and Brunauer–Emmett–Teller (BET) isotherms (see Table 2).



Fig. 1. Chemical structure of DR 80 dye.

Table 2  
Linearised isotherm coefficients for adsorption of DR 80 dye on almond shells

Adsorbent type	Langmuir isotherm			Freundlich isotherm			BET isotherm		
	$Q_0$	$K_L$	$R_1^2$	$K_F$	$n$	$R_2^2$	$K_b$	$q_m$	$R_3^2$
Mixture shells	28.50	1.821	<b>0.9624</b>	15.563	7.353	0.8809	-4.6621	1.3199	0.9604
External shells	23.753	0.494	0.9158	11.951	5.163	<b>0.9715</b>	-7.84	6.378	0.8639
Internal shells	22.00	0.099	0.9641	8.168	2.145	0.9629	-65.556	16.949	<b>0.9893</b>

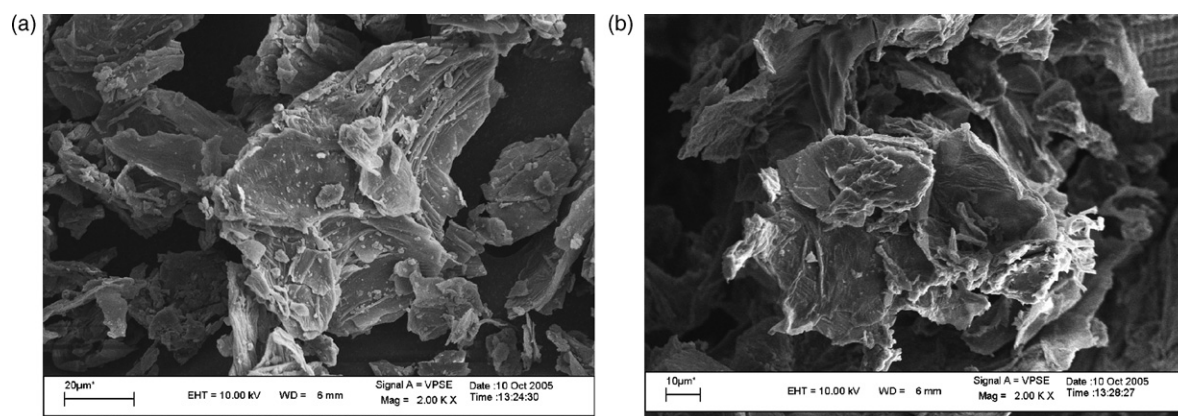


Fig. 2. Scanning electron micrographs of the internal almond shells: (a) without adsorption and (b) after 1440 min adsorption.

Scanning electron microscopic (SEM) images of the surface of the almond shells were obtained using LEO 1455VP scanning microscope for internal shells (Fig. 2), external shells (Fig. 3) and mixture shells (Fig. 4). These pictures show the surface of the adsorbent prior to adsorption process (Figs. 2a, 3a and 4a) and after adsorption experiments (Figs. 2b, 3b and 4b). The

SEM photographs of the original almond shells (Figs. 2a, 3a and 4a) show that the whole shells have a rough surface with almost non-compact structure. It is obvious that the almond shells have considerable numbers of pore spaces where appropriate conditions exist for DR 80 dye to be trapped and adsorbed into these pores. (Figs. 2b, 3b and 4b) illustrate that the DR 80

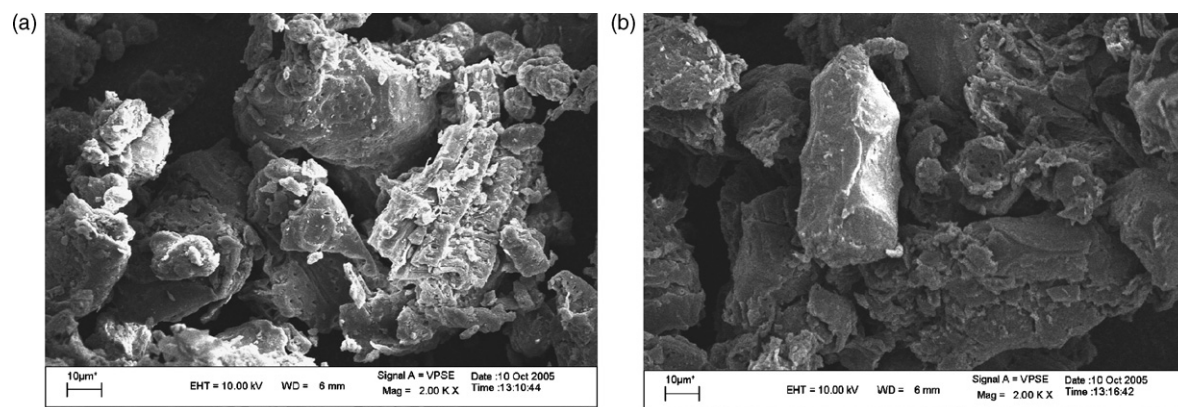


Fig. 3. Scanning electron micrographs of the external almond shells: (a) without adsorption and (b) after 1440 min adsorption.

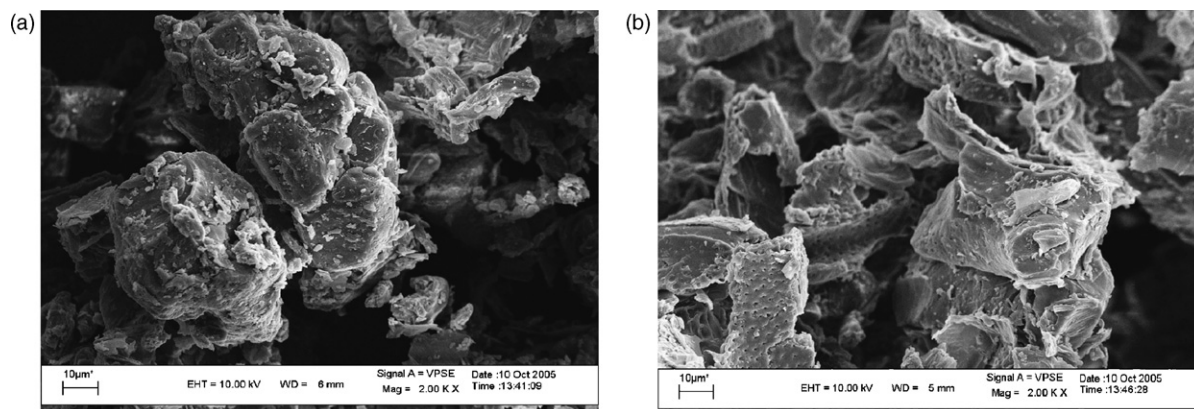


Fig. 4. Scanning electron micrographs of the mixture almond shells: (a) without adsorption and (b) after 1440 min adsorption.

dye is homogeneously adsorbed on the surfaces of the almond shells.

### 3. Results and discussion

#### 3.1. Analysis of the samples

A CECIL 2021 spectrophotometer was used at the maximum wavelength ( $\lambda_{\max}$ ) of 542.5 nm to make the absorbance measurements. An FTIR analysis was performed in the range of 450–4000  $\text{cm}^{-1}$  in order to explore the surface characteristics of the adsorbent. Fig. 5 shows the FTIR spectrum of almond shells. The peak positions showing major adsorption bands were observed at 3432.13, 2927.96, 1741.26, 1633.20, 1382.18, 1252.68, 1053.85 and 602.93  $\text{cm}^{-1}$ . The band at 3432.13  $\text{cm}^{-1}$  is due to stretch vibration (O–H), The band at 2927.96 may represent the C–H aromatic and aliphatic stretch vibration, the band at 1633.20  $\text{cm}^{-1}$  represents the carbonyl group stretching, the band at 1382.18  $\text{cm}^{-1}$  is due to C–H deformation vibration, the band at 1053.85  $\text{cm}^{-1}$  reflects the C–O stretch vibration and the band at 602.93  $\text{cm}^{-1}$  may correspond to SiO–H vibration.

The surface area of the mixture type of almond shell was determined by BET method. In this investigation, the value 10.5  $\text{m}^2/\text{g}$  was calculated for its surface area.

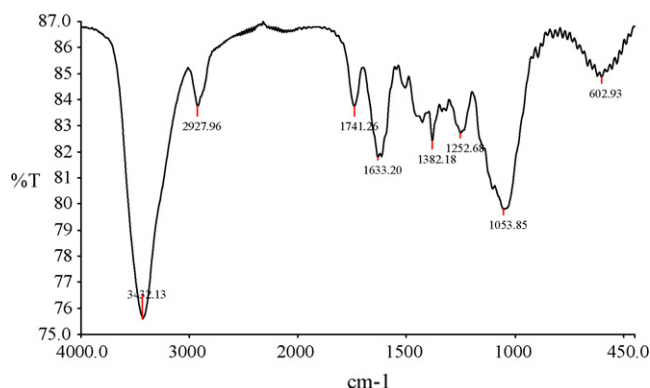


Fig. 5. The FTIR spectrum of almond shells.

#### 3.2. Adsorption isotherms

Adsorption isotherms describe how adsorbates interact with adsorbents and are crucial in optimizing the use of adsorbents. Adsorption isotherms demonstrate the relationships between equilibrium concentrations of adsorbate in the solid phase  $q$ , and in the liquid phase  $C$  at constant temperature [5].

Adsorption isotherms are described in many mathematical forms. They are often obtained in the laboratory using batch tests in which the equilibrium data are attempted by various isotherm models such as Langmuir, Freundlich [5,11,30] and Brunauer–Emmett–Teller (BET) [29] isotherms.

The Langmuir isotherm has been widely used to describe single-solute systems. This isotherm assumes that intermolecular forces decrease rapidly with distance and consequently it can predict monolayer coverage of the adsorbate on the outer surface of the adsorbent. Further assumption is that adsorption occurs at specific homogeneous sites within the adsorbent and there is no significant interaction among adsorbed species. The Langmuir isotherm is given by the following equation:

$$q_e = \frac{Q_0 K_L C_e}{1 + K_L C_e} \quad (1)$$

where  $q_e$  is the solid phase dye concentration at equilibrium (mg/g),  $C_e$  the equilibrium concentration of dye (mg/L),  $Q_0$  denotes the maximum adsorption capacity (mg/g) and  $K_L$  is the Langmuir isotherm constant (L/mg).

A linear expression for the Langmuir isotherm is:

$$\frac{C_e}{q_e} = \frac{1}{Q_0 K_L} + \frac{1}{Q_0} (C_e) \quad (2)$$

If  $C_e/q_e$  is plotted against  $C_e$  gives a straight line with a slope of  $1/Q_0$  and an intercept of  $1/(Q_0 K_L)$ .

In this study, Freundlich expression was also applied for the adsorption of DR 80 dye on almond shells. This empirical expression is used to describe heterogeneous systems [31]. The Freundlich isotherm equation is given as:

$$q_e = K_F C_e^{1/n} \quad (3)$$

where  $C_e$  is the equilibrium concentration of dye (mg/L),  $K_F$  and  $n$  are Freundlich isotherm constants indicating the extend of

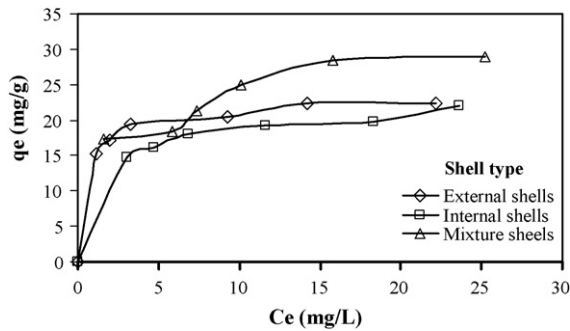


Fig. 6. Adsorption isotherms for the adsorption of DR 80 dye by almond shells. Conditions. pH 6,  $T = 20 \pm 1$  °C, agitating speed = 200 rpm.

the adsorption and the degree of non-linearity between solution concentration and adsorption, respectively.

The third isotherm equation used in this study is the Brunauer–Emmett–Teller (BET) isotherm [29]. The linear form of this model is written as:

$$\frac{C_e}{(C_s - C_e)q_e} = \frac{1}{K_b q_m} + \left( \frac{K_b - 1}{K_b q_m} \right) \left( \frac{C_e}{C_s} \right) \quad (4)$$

where  $C_s$  is the saturation concentration of dye (mg/L),  $q_m$  the amount of dye adsorbed in forming a complete monolayer (mg/g), and  $K_b$  is the constant describing the energy of interaction with the surface.

The equilibrium isotherms for the adsorption of DR 80 dye on almond shells determined for the initial concentrations of 50 mg/L are shown in Fig. 6.

The empirical parameters of the Langmuir, Freundlich and BET isotherms determined for internal, external and mixture almond shells are given in Table 2.

As this table shows, for mixture shells adsorbent the correlation coefficient,  $R^2$ , for the Langmuir isotherm is 0.9624. This value is greater than those  $R^2$  values calculated for the Freundlich and Brunauer–Emmett–Teller (BET) isotherms. This means that the adsorption process of DR 80 dye on mixture almond shells adsorbent could be well described by the Langmuir isotherm model. In the case of internal shells adsorbent, the correlation coefficient for the BET isotherm is the highest value equal to 0.9893. For external shells, the Freundlich isotherm has the maximum correlation coefficient ( $R^2 = 0.9715$ ). These suggest that

the adsorption of DR 80 dye on internal shells is explained by BET isotherm and the adsorption of this dye on external shells is described by Freundlich isotherm model.

### 3.3. Adsorption kinetics

It is essential to predict the rate at which dye is removed from aqueous solutions in order to design an appropriate treatment system based on adsorption process.

The adsorption kinetics can be described using a pseudo-first order and a pseudo-second-order model. The pseudo-first order model can be represented by the following Lagergren's expression:

$$\log(q_1 - q_t) = \log q_1 - \frac{K_{1,ad}}{2.303}(t) \quad (5)$$

where  $q_1$  is the amount of dye adsorbed at equilibrium (mg/g),  $q_t$  the amount of dye adsorbed at time  $t$  (mg/g),  $K_{1,ad}$  the pseudo-first-order rate constant (1/min) and  $t$  is the time (min).

The rate of pseudo-second-order model depends on the amount of dye adsorbed on the surface of adsorbent and the quantity adsorbed at equilibrium [32]. This model can be given as follows [33]:

$$\frac{t}{q_t} = \frac{1}{K_{2,ad}q_e^2} + \frac{1}{q_e}(t) \quad (6)$$

where  $K_{2,ad}$  is the rate constant of the pseudo-second-order model (g/mg min) and  $q_e$  is the amount of the dye adsorbed at equilibrium (mg/g).

The kinetics parameters of the pseudo-first-order and pseudo-second-order models at different initial concentrations of DR 80 dye are given in Table 3 for various types of adsorbents.

As Table 3 shows, the correlation coefficients,  $R^2$  for the pseudo-first-order model varies from 0.8188 (mixture shells and for an initial dye concentration of 100 mg/L) to 0.9697 (mixture shells and for an initial dye concentration of 150 mg/L) and for the pseudo-second-order model this coefficient varies from 0.9986 (internal shells and for an initial dye concentration of 100 mg/L) to 1 (mixture shells, and for an initial dye concentration of 50 mg/L). The extremely high value of  $R^2$  for pseudo-second-order model for all adsorbent types and at any initial dye concentration suggests that the adsorption system for

Table 3  
Kinetics constants for DR 80 obtained at pH 6

Adsorbent type	Initial concentration (mg/L)	Pseudo-first-order			Pseudo-second-order		
		$q_1$ (mg/g)	$K_{1,ad}$ (1/min)	$R^2$	$q_e$ (mg/g)	$K_{2,ad}$ (g/mg min)	$R^2$
Internal shells	50	5.27	$5.30 \times 10^{-3}$	0.9394	13.48	$1.41 \times 10^{-2}$	0.9978
	100	7.93	$7.83 \times 10^{-3}$	0.9619	23.26	$1.03 \times 10^{-2}$	0.9986
	150	6.92	$1.08 \times 10^{-2}$	0.8902	26.04	$1.24 \times 10^{-2}$	0.9995
External shells	50	4.23	$5.99 \times 10^{-3}$	0.9508	15.02	$1.88 \times 10^{-2}$	0.9994
	100	6.98	$1.24 \times 10^{-2}$	0.8432	34.25	$1.42 \times 10^{-2}$	0.9993
	150	13.57	$1.61 \times 10^{-2}$	0.9559	50.25	$6.69 \times 10^{-3}$	0.9998
Mixture shells	50	2.44	$1.04 \times 10^{-2}$	0.9020	20.04	$3.71 \times 10^{-2}$	0.9999
	100	11.49	$1.87 \times 10^{-2}$	0.8188	39.22	$9.81 \times 10^{-4}$	0.999
	150	16.05	$1.61 \times 10^{-2}$	0.9697	52.63	$5.286 \times 10^{-3}$	0.9995

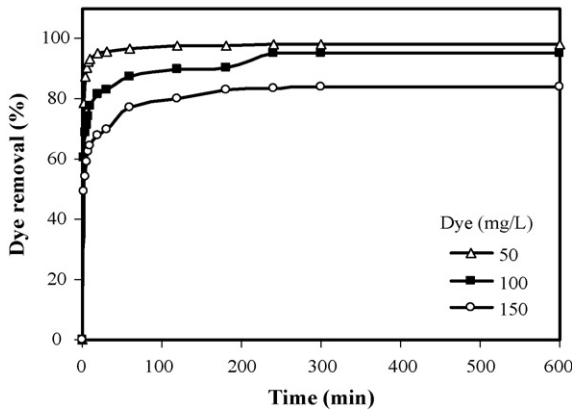


Fig. 7. Effect of contact time and dye concentration on the percentage removal of DR 80 dye. Conditions: pH 6, T = 20 ± 1 °C, agitating speed = 200 rpm, shell type = mixture.

DR 80 removal using almond shells can be well described by pseudo-second-order kinetics model. Moreover, an increase in the initial dye concentration reduced kinetics of DR 80 dye sorption. However, this reduction is less obvious for internal shell type.

3.4. Effect of contact time and dye concentration

The adsorption efficiency of DR 80 dye on almond shells was evaluated as a function of contact time and initial dye concentration. A mixture type of almond shell was selected for this experiment. The initial dye concentration was varied from 50 to 150 mg/L. The result is shown in Fig. 7.

As Fig. 7 shows, the percentage removal of DR 80 dye was rapid at the beginning of the adsorption process and gradually decreased as time progressed to attain equilibrium after 300 min. The percentage removal of dye reached to about 94% at equilib-

rium time. It is evident from Fig. 7 that the percentage removal of DR 80 dye remained constant above time 300 min to time about 1500 min of adsorption process.

It is also observed from the figure that the percentage removal of DR 80 dye decreased from 94 to 83.9% at equilibrium as dye concentrations increased from 50 to 150 mg/L.

3.5. Effect of shell type

Fig. 8 shows the effect of shell type on the percentage removal of DR 80 dye from solution phase for three different shells including internal, external and mixture. Initial dye concentration was changed from 50 to 150 mg/L. The result indicates that for an initial dye concentration of 50 mg/L (Fig. 8a), all shell types showed almost same effect on the percentage removal of DR 80 dye from the aqueous solution with a maximum removal of 97% for external type, and a minimum removal of 80% for internal shell type after 1 h of the adsorption process. As initial dye concentration increased from 50 to 100 mg/L (Fig. 8b), the effect of external and mixture shells for the removal of DR 80 dye is quite close. The internal shells showed different results in the percentage removal of dye. Less amount of DR 80 dye was removed from the aqueous solution using internal shells.

As it is evident from Fig. 8b, after a process time of 1 h, the percentage removal of DR 80 dye for external shells is about 91%. Furthermore, this value for the mixture shells is about 87%, but the percentage removal rate for internal shells is about 58%. The effect of shell type on the adsorption process is more obvious when the initial dye concentration increased to 150 mg/L. The external shell type showed to be an effective adsorbent for the removal of DR 80 dye from the aqueous solution with a percentage removal of about 87% after a process time of 1 h. The percentage removal values of 77.5 and 45.5% were obtained for mixture and internal shell types, respectively.

Table 4 Pseudo first- and second-order kinetics constants of DR 80 dye at different pH, various adsorbent types, and given for an initial dye concentration of 50 mg/L

Adsorbent type	pH	First-order kinetic constants			Second-order kinetic constants		
		q <sub>e</sub>	K <sub>1,ad</sub>	R <sup>2</sup>	q <sub>e</sub>	K <sub>2,ad</sub>	R <sup>2</sup>
Internal shells	2	4.15	7.369 × 10 <sup>-3</sup>	0.9165	15.82	0.0195	0.9996
	4	5.39	4.606 × 10 <sup>-3</sup>	0.9286	13.28	0.0151	0.9982
	6	5.27	5.297 × 10 <sup>-3</sup>	0.9394	13.48	0.0141	0.9978
	8	4.94	4.836 × 10 <sup>-3</sup>	0.9102	13.14	0.0166	0.9980
	10	5.29	5.067 × 10 <sup>-3</sup>	0.9264	13.46	0.0147	0.9982
	12	5.06	4.836 × 10 <sup>-3</sup>	0.9745	13.21	0.0145	0.9980
External shells	2	3.64	7.83 × 10 <sup>-3</sup>	0.9348	16.56	0.0224	0.9997
	4	4.32	5.29 × 10 <sup>-3</sup>	0.8463	14.54	0.0212	0.9996
	6	4.23	5.99 × 10 <sup>-3</sup>	0.9508	15.02	0.0188	0.9994
	8	4.42	5.76 × 10 <sup>-3</sup>	0.9336	14.47	0.0181	0.9993
	10	4.30	5.76 × 10 <sup>-3</sup>	0.9253	14.56	0.0188	0.9992
	12	4.28	5.76 × 10 <sup>-3</sup>	0.9779	14.21	0.0163	0.9987
Mixture shells	2	1.40	1.59 × 10 <sup>-2</sup>	0.9104	20.49	0.0773	1
	4	1.968	9.673 × 10 <sup>-3</sup>	0.8159	20.00	0.0519	1
	6	2.44	1.04 × 10 <sup>-2</sup>	0.902	20.04	0.0371	0.9999
	8	1.993	1.17 × 10 <sup>-2</sup>	0.8794	19.65	0.0494	1
	10	1.76	7.139 × 10 <sup>-3</sup>	0.7909	19.23	0.0612	1
	12	2.317	5.297 × 10 <sup>-3</sup>	0.7266	18.18	0.0534	1

The main reason for the lower dye removal yield of the internal shells which decreases as initial dye concentration increases, is that the internal shells are more compact and less porous than the external shells.

### 3.6. Effect of pH

The pH of the dye solution plays an important role on the adsorption capacity. The variation of DR 80 adsorption on almond shells over a broad range of pH is illustrated in Fig. 9. As shown, at any pH, the adsorption of DR 80 on mixture type

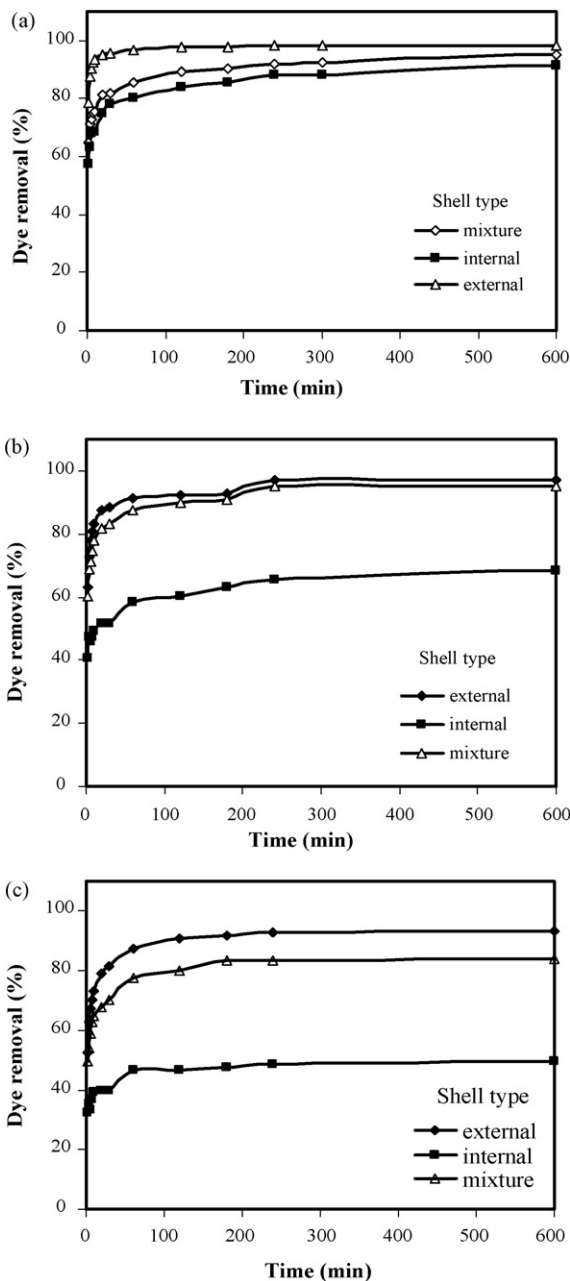


Fig. 8. Effect of almond shell type on the percentage removal of DR 80 dye. Conditions: pH 6, agitating speed = 200 rpm,  $T = 20 \pm 1^\circ\text{C}$ : (a) initial dye concentration: 50 mg/L, (b) initial dye concentration: 100 mg/L and (c) initial dye concentration: 150 mg/L.

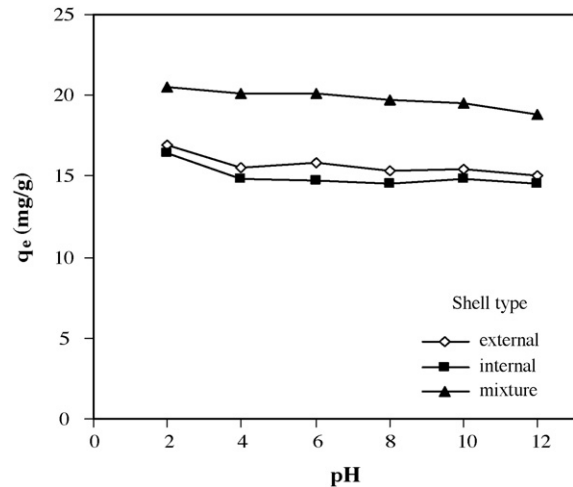


Fig. 9. Effect of pH on DR 80 dye adsorption on almond shells. Conditions:  $T = 20 \pm 1^\circ\text{C}$ , agitating speed = 200 rpm, particle size  $\leq 0.125$  mm.

of the almond shell shows higher adsorption capacity than that on external and internal shells. It is clear from the figure that, for mixture type, the adsorption decreased linearly from 20.5 to 18.8 mg/g when pH increased from 2 to 12. Other types of the almond shell show almost a similar trend. As illustrated well, the adsorption capacity of internal and external shells for the adsorption of DR 80 dye is almost same. The amount of dye adsorbed decreased as the pH of the dye solution increased from 2 to 4. Above pH 4 until pH 12, the adsorption of dye decreased again but at a lower rate. The maximum adsorption capacity of different types of almond shells (20.5, 16.96 and 16.4 mg/g for mixture, external and internal shells) was obtained at pH 2. Because the pH variations showed no considerable change on the maximum adsorption capacity, for this reason, pH 6 was therefore selected for all other experiments.

The kinetics parameters of the pseudo-first-order and pseudo-second-order models at different pH of the dye solution are given in Table 4 for various types of adsorbents and for an initial dye concentration of 50 mg/L. These parameters were obtained from the Lagergren and Ho and McKay plots. As shown in Table 4, at any pH and for all types of adsorbent, the high values of correlation coefficients showed that the kinetics data conformed well to the pseudo-second-order kinetic model.

## 4. Conclusions

The study presented revealed that almond shells could be effectively used to remove DR 80 dye from an aqueous solution. The effect of shell type on the percentage removal of DR 80 dye was examined. The result indicated that for an initial dye concentration of 50 mg/L, all shell types showed almost same effect on the percentage removal of DR 80 dye from the aqueous solution with a maximum removal of 97% for external type, and a minimum removal of 80% for internal shell type after 1 h of the adsorption process. It was found that the adsorption process by mixture almond shells adsorbent could be well described by the Langmuir isotherm. While the internal and the external shells follow BET and Freundlich sorption isotherm models, respec-

tively. Furthermore, a pseudo-second-order kinetics showed to be well suited with the rate of sorption. Although, the generation of effluents containing direct dyes by textile industry is almost unavoidable, the results of the experimental studies can help to design an appropriate remediation plan to minimise the unfavourable impacts caused by industrial effluents.

### Acknowledgements

The authors greatly acknowledge the financial help provided by the Iran Colour Research Centre (ICRC) and thank Shahrood University of Technology, for supporting this research.

### References

- [1] D. Georgiou, P. Melidis, A. Aivasidis, K. Gimouhopoulos, Degradation of Azo-reactive dyes by ultraviolet radiation in the presence of hydrogen peroxide, *Dyes Pigments* 52 (2002) 69–78.
- [2] L.S. Tsui, W.R. Roy, M.A. Cole, Removal of dissolved textile dyes from wastewater by a compost sorbent, *Coloration Technol.* 119 (2003) 14–18.
- [3] R. Gong, Y. Ding, M. Li, C. Yang, H. Liu, Y. Sun, Utilization of powdered peanut hull as biosorbent for removal of anionic dyes from aqueous solution, *Dyes Pigments* 64 (2005) 187–192.
- [4] S. Venkata Mohan, P. Sailaja, M. Srimurali, J. Karthikeyan, Color removal of monoazoacid dye from aqueous solution by adsorption and chemical coagulation, *Environ. Eng. Policy* 1 (1999) 149–154.
- [5] V. Gokmen, A. Serpen, Equilibrium and kinetic studies on the adsorption of dark colored compounds from apple juice using adsorbent resin, *J. Food Eng.* 53 (2002) 221–227.
- [6] K.R. Ramakrishna, T. Viraraghavan, Use of slag for dye removal, *Waste Manag.* 17 (8) (1997) 483–488.
- [7] C. Hachem, F. Bocquillon, O. Zahraa, M. Bouchy, Decolorization of textile industry wastewater by the photocatalytic degradation process, *Dyes Pigments* 49 (2001) 117–125.
- [8] G. Annadurai, R.S. Juang, D.J. Lee, Factorial design analysis for adsorption of dye on activated carbon beads incorporated with calcium alginate, *Adv. Environ. Res.* 6 (2002) 191–198.
- [9] D. Mohan, K.P. Singh, G. Singh, K. Kumar, Removal of dyes from wastewater using fly ash, a low-cost adsorbent, *Ind. Eng. Chem. Res.* 41 (15) (2002) 3688–3695.
- [10] M. Neamtu, C. Zaharia, C. Catrinescu, A. Yediler, M. Macoveanu, A. Ketrup, Fe-exchanged Y zeolite as catalyst for wet peroxide oxidation of reactive azo dye Procion Marine H-EXL, *Appl. Catal. B Environ.* 48 (2004) 287–294.
- [11] S. Chakraborty, S. De, S. DasGupta, J.K. Basu, Adsorption study for the removal of a basic dye: experimental and modeling, *Chemosphere* 58 (2005) 1079–1086.
- [12] N.M. Mahmoodi, M. Arami, N. Yousefi Limaee, N. Salman Tabrizi, Decolorization and aromatic ring degradation kinetics of Direct Red 80 by UV oxidation in the presence of hydrogen peroxide utilizing TiO<sub>2</sub> as a photocatalyst, *Chem. Eng. J.* 112 (2005) 191–196.
- [13] H. Chun, W. Yizhong, Decolorization and biodegradability of photocatalytic treated azo dyes and wool textile wastewater, *Chemosphere* 39 (1999) 2107–2115.
- [14] J. Wu, M.A. Eiteman, S.E. Law, Evaluation of membrane filtration and ozonation processes for treatment of reactive dye wastewater, *J. Environ. Eng.* 124 (1998) 272–277.
- [15] C.L. Pearce, J.R. Lloyd, J.T. Guthrie, The removal of colour from textile wastewater using whole bacterial cells: a review, *Dyes Pigments* 58 (2003) 179–196.
- [16] A.G. Vlyssides, M. Loizidou, P.K. Karlis, A.A. Zorpas, D. Papaioannou, Electrochemical oxidation of a textile dye wastewater using a Pt/Ti electrode, *J. Hazard. Mater.* 70 (1999) 41–52.
- [17] G. Atun, G. Hisarli, W.S. Sheldrich, M. Muhler, Adsorptive removal of methylene blue from colored effluents on fuller's earth, *J. Colloid Interf. Sci.* 261 (2003) 32–39.
- [18] Z. Aksu, Application of biosorption for the removal of orange pollutants: a review, *Process Biochem.* 40 (2005) 997–1026.
- [19] M. Arami, N. Yousefi Limaee, N.M. Mahmoodi, N. Salman Tabrizi, Removal of dyes from colored textile wastewater by orange peel adsorbent: equilibrium and kinetic studies, *J. Colloid Interf. Sci.* 288 (2005) 371–376.
- [20] V.K. Garg, M. Amita, R. Kumar, R. Gupta, Basic dye (methylene blue) removal from simulated wastewater by adsorption using Indian rosewood sawdust: a timber industry waste, *Dyes Pigments* 63 (2004) 243–250.
- [21] J. Pavel, H. Buchtova, M. Ryznarova, Sorption of dyes from aqueous solutions onto fly ash, *Water Res.* 37 (2003) 4938–4944.
- [22] T. Robinson, B. Chandra, P. Nigam, Removal of dyes from a synthetic textile dye effluent by biosorption on apple pomace and wheat straw, *Water Res.* 36 (2002) 2824–2830.
- [23] Y. Fu, T. Viraraghavan, Removal of Congo red from an aqueous solution by fungus *Aspergillus Niger*, *Adv. Environ. Res.* 7 (2002) 239–247.
- [24] M. Arami, N. Yousefi Limaee, N.M. Mahmoodi, N. Salman Tabrizi, Equilibrium and kinetics studies for the adsorption of direct and acid dyes from aqueous solution by soy meal hull, *J. Hazard. Mater.* 135 (1–3) (2006) 171–179.
- [25] M. Arami, N. Yousefi Limaee, N.M. Mahmoodi, Investigation on the adsorption capability of egg shell membrane towards model textile dyes, *Chemosphere* 65 (11) (2006) 1999–2008.
- [26] R.R. Bansode, J.N. Lasso, W.E. Marshall, R.M. Rao, R.J. Portier, Adsorption of volatile organic compounds by pecan shell and almond shell-based granular activated carbons, *Bioresource Technol.* 90 (2003) 175–184.
- [27] A.A.M. Daifullah, B.S. Girgis, Impact of surface characteristics of activated carbon on adsorption of BTEX, *Colloids Surf. A: physicochem. Eng. Aspects* 214 (2003) 181–193.
- [28] B.N. Estevinho, N. Ratola, A. Alves, L. Santos, Pentachlorophenol removal from aqueous matrices by sorption with almond shell residues, *J. Hazard. Mater.* B137 (2006) 1175–1181.
- [29] R. Shawabkeh, A. Al-Harashsheh, A. Al-Otoom, Copper and zinc sorption by treated oil shale ash, *Sep. Purif. Technol.* 40 (2004) 251–257.
- [30] O. Nitzsche, H. Vereecken, Modeling sorption and exchange processes in column experiments and large scale field studies, *Mine Water Environ.* 21 (2002) 15–23.
- [31] S. Wang, Y. Boyjoo, A. Choueib, Z.H. Zhu, Removal of dyes from aqueous solution using fly ash and red mud, *Water Res.* 39 (1) (2005) 129–138.
- [32] A. Gucek, S. Sener, S. Bilgen, M.L. Mazmanci, Adsorption and kinetic studies of cationic and anionic dyes on pyrophyllite from aqueous solutions, *J. Colloid Interf. Sci.* 286 (2005) 53–60.
- [33] Y.S. Ho, G. McKay, Sorption of dye from aqueous solution by peat, *Chem. Eng. J.* 70 (2) (1998) 115–124.